Energy Conversion and Management 126 (2016) 342–351

Contents lists available at ScienceDirect

Energy Conversion and Management

journal homepage: www.elsevier.com/locate/enconman

Heat transfer measurement in a three-phase spray column direct contact heat exchanger for utilisation in energy recovery from low-grade sources

Ali Sh. Baqir [a], Hameed B. Mahood [b,*], Mudher S. Hameed [b], Alasdair N. Campbell [c]

[a] Al-Furat Al-Awsat Technical University, Al-Najaf Engineering Technical College, Department of Aeronautical Engineering, Al-Najaf, Iraq
[b] University of Misan, Misan, Iraq
[c] Department of Chemical and Process Engineering, University of Surrey, UK

ARTICLE INFO

Article history:
Received 11 June 2016
Received in revised form 26 July 2016
Accepted 8 August 2016

Keywords:
Spray column three-phase direct contact heat exchanger
Local volumetric heat transfer coefficient
Active height
Sparger configuration

ABSTRACT

Energy recovery from low-grade energy resources requires an efficient thermal conversion system to be economically viable. The use of a liquid-liquid-vapour direct contact heat exchanger in such processes could be suitable due to their high thermal efficiency and low cost in comparison to a surface type heat exchanger.

In this paper, the local volumetric heat transfer coefficient (U_v) and the active height (H_v) of a spray column three-phase direct contact heat exchanger (evaporator) have been investigated experimentally. The heat exchanger comprised a cylindrical Perspex tube of 100 cm height and 10 cm diameter. Liquid pentane at its saturation temperature and warm water at 45 °C were used as the dispersed phase and the continuous phase respectively. Three different dispersed phase flow rates (10, 15 and 20 L/h) and four different continuous phase flow rates (10, 20, 30 and 40 L/h) were used throughout the experiments. In addition, three different sparger configurations (7, 19 and 36 nozzles) with two different nozzle diameters (1 and 1.25 mm) were tested. The results showed that the local volumetric heat transfer coefficient (U_v) along the column decreases with height. An increase in both the continuous and dispersed phase flow rates had a positive effect on U_v, while an increase in the number of nozzles in the sparger caused U_v to decrease. The active height was significantly affected by the dispersed and continuous phase flow rates, the sparger configuration and the temperature driving force in terms of the *Jacob* number.

1. Introduction

Population growth and the continuing deployment and development of technology around the word require augmentation of energy supplies. Currently, fossil fuels provide about 80% of the gross energy needed. Only 11% of the total energy required is generated from renewable energy resources [1]. Therefore, many environmental problems, such as air pollution and global warming may continue to accelerate. Such problems necessitate novel solutions. Accordingly, heat recovery processes, especially those that exploit industrial and interfacial low-grade energy resources, have received an increasing amount of attention. There are, however, many obstacles still hindering the development of these processes. In particular, the low thermal efficiency of the equipment used, and specifically the heat exchanger, must be overcome. The high capital cost of the heat exchanger can also significantly affect the feasibility of the heat recovery plant. The low heat exchanger efficiency is principally due to the presence of metallic barriers that separate the hot and cold fluid streams. These surfaces impose an additional, potentially large, heat transfer resistance and are prone to corrosion and fouling. Consequently, the heat transfer efficiency of the heat exchanger will reduce with time.

These problems could be mitigated by using direct contact heat exchangers. The absence of the internal separating wall between the fluid streams in the direct contact heat exchanger results in many advantages over the traditional surface type heat exchanger. For example, the direct contact device can be operated with a very low temperature difference between the working fluids, even as low as $\Delta T = 1$ °C. The fouling and corrosion problems are all but eliminated, as there is no heat transfer surface, and there is an increase in the heat transfer rate between the fluids. Finally, the direct contact exchanger has a low capital and operational cost as it can be constructed from very cheap materials [2]. In this context, Wright [3] found that the replacement of a surface type heat exchanger that was used in a 5 MW power plant by a direct contact heat exchanger could reduce the capital cost of the plant by 25%. For these reasons, the direct contact heat exchanger, especially

* Corresponding author.
E-mail address: hbmahood@yahoo.com (H.B. Mahood).

http://dx.doi.org/10.1016/j.enconman.2016.08.013
0196-8904/

Nomenclature

A	cross-sectional area of column, m^2
C_{pc}	specific heat of continuous phase, kJ/kg K
Ja_c	Jacobs number
h_{fg}	latent heat of condensation, kJ/kg
H_v	active height of heat exchanger, m
$\dot{m}_d$	dispersed phase mass flow rate, kg/min
$\dot{m}_c$	continuous phase mass flow rate, kg/min
nz	number of nozzle in the sparger
q	heat transfer rate, kW
Q_c	volumetric flow rate of the continuous phase, L/h
Q_d	volumetric flow rate of the dispersed phase, L/h
Re_o	nozzles' Reynolds number
T_c	temperature of the continuous phase, °C
T_d	temperature of the dispersed phase, °C
ΔT_{lm}	log-mean temperature difference, °C
U	relative velocity, m/s
U_v	volumetric heat transfer coefficient, kW/m^3 K
V_r	radial velocity component, rad
V_θ	tangential velocity component, rad
Z	axial position, m
ΔZ	sub-height along column, m

Greek symbols

ρ_c	density of continuous phase, kg/m^3
ρ_v	density of dispersed phase vapour, kg/m^3
θ	angle, rad

Subscripts

c	continuous phase
d	dispersed phase
i	initial, or location
o	outlet

the three-phase direct contact heat exchanger, has received considerable attention in many recent experimental and theoretical investigations. These investigations were presented within the context many different industrial processes, such as water desalination, power generation from geothermal energy and heat recovery from low-grade energy resources [4,5].

It has been shown previously [6,7] that the heat transfer characteristics of the spray column heat exchanger can be represented clearly by the volumetric heat transfer coefficient. Despite this, only a limited number of studies have actually reported the volumetric heat transfer coefficient. Bauerle and Ahlert [8] observed an increase in the volumetric heat transfer coefficient of the spray column heat exchanger with dispersed phase hold-up until the flooding limit of the exchanger was reached. There was a subsequent decline in heat transfer coefficient. The same trend in the volumetric heat transfer coefficient in a spray column heat exchanger was noted by Plass et al. [9]. Their results were correlated and accurately fitted with the data over a range of hold-ups. The effect of the initial diameter of the dispersed phase droplets can significantly affect the volumetric heat transfer coefficient in the spray column direct contact heat exchanger, by affecting the interfacial heat transfer area. Sideman et al. [10] ascertained that there is a decrease in the volumetric heat transfer coefficient of the spray column heat exchanger with an increase in the initial drop diameter. This observation was confirmed numerically by Cabon and Boehm [11] and Jacobs and Golafshani [12].

There are few analytical models for the volumetric heat transfer coefficient available in the literature. Only that of Mori [7] is prominent. The difficulty in deriving and solving analytical models is because of the complexity that arises due to the large number of interacting parameters that control the heat transfer in the spray column. However, Mori [7] was able to exploit the expression for the heat transfer coefficient for single drop evaporating in an immiscible liquid [13] as a starting point for his analytical solution. He succeeded in finding both the local and the average volumetric heat transfer coefficient of the spray column direct contact heat exchanger.

In contrast to the few studies that have investigated the volumetric heat transfer coefficient, much research has been directed toward the temperature distribution along the spray column direct contact heat exchanger, both experimentally and theoretically [14–17,11,12,18]. All of these studies have confirmed that the exit temperature of the dispersed phase increased with exchanger height, while it decreases in the case of the continuous phase. Interestingly, and surprisingly, Siqueiros and Bonilla [19] observed that when the initial temperature (inlet temperature) of the continuous phase (water) ranged between 75 and 88 °C and the inlet temperature of the dispersed phase (pentane) between 23 and 38 °C, the continuous phase outlet temperature was between 70 and 84 °C and the dispersed phase outlet temperature between 72 and 85 °C. Although, no other study has confirmed these results, they are in accord with the expectation that latent heat controls the direct contact heat exchange process. Recently, Mahood et al. [20] studied analytically the distribution of the temperature of both the dispersed and continuous phases along a spray column direct contact condenser. The temperature of the dispersed phase was shown to increase with exchanger height and with decreasing drop size. Wang et al. [21] found that the volumetric heat transfer calculated in respect to the dispersed-continuous phase temperature interface was significantly greater than that calculated based on the average dispersed phase-continuous phase bulk temperature difference. Recently, Jiang et al. [22] noted that the size of a spray column direct contact heat exchanger could be considerably reduced when using packed materials, as the volumetric heat transfer coefficient was significantly increased. Mahood et al. [1,4,23–29] investigated the heat transfer characteristics of a bubble type three-phase direct contact condenser. Different effective parameters, such as the mass flow rates of the dispersed and continuous phases, and the initial temperature of the dispersed phase on the transient [4] and steady state temperature distributions along the condenser [23], the transient [24] and steady volumetric heat transfer coefficient [25], the condenser efficiency and ultimately cost were studied [1]. In addition, the conditions under which the direct contact condenser flooded and its heat transfer performance under these conditions were determined [26]. Furthermore, the feasibility of implementing the three-phase direct contact heat exchanger in the applications of water desalination and power generation was investigated [27,28]. Finally, a new model for the drag coefficient exerted on the bubbles as they move through a real three-phase exchanger was developed [29]. More recently Baqir et al. [30] measured the average volumetric transfer coefficient and the dispersed phase holdup in a liquid-liquid-vapour heat exchanger. The effect of the initial drop size, the heat exchanger active height, and the sparger configuration on the average volumetric heat transfer coefficient was tested. They observed that average volumetric heat transfer coefficient was significantly

affected by the change in the drop size, the holdup ratio and the heat exchanger active height. On the other hand, the sparger configuration had a very slight impact.

In the present study, measurements of the local volumetric heat transfer coefficient along and the active height of the three-phase direct contact evaporator were carried out. The effect of the continuous phase flow rate, the dispersed phase flow rate, the sparger configuration and the diameter of the injection nozzles on the volumetric heat transfer coefficient and the active height were examined.

2. Experimental work

2.1. Experimental setup

In Fig. 1 is shown a schematic diagram of the experimental rig that was used in the present work. The apparatus is comprised of the direct contact column (test section), dispersed phase supply system, continuous phase supply system, measuring devices and auxiliary equipment, such as the data logger and thermocouples. The direct contact column (test section) consists of a 100 cm long cylindrical Perspex tube with a 10 cm diameter. Six equidistant holes along the test section were made to fix six calibrated K-type thermocouples (average error ±1 °C). A circular shaped sparger with an outer diameter of 49 cm is fixed at the bottom of the column. Three different sparger configurations (7 nozzles, 19 nozzles and 36 nozzles), with two different nozzle diameters were used during the experiments. In Fig. 2 is presented a schematic diagram of the sparger configurations. The test section is connected to the dispersed and continuous phase supplies via inlet tubes from its bottom and top respectively. The dispersed phase supply unit comprises a 20 L plastic storage tank, peristaltic pump, pipes, fittings and valves. Liquid pentane (99% purity) was used as the dispersed phase. Table 1 shows the properties of pentane at 1 bar and saturation temperature.

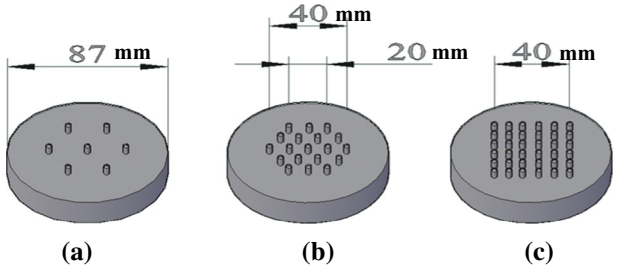

Fig. 2. Sparger configurations used in the present work. Specifically, spargers with (a) 7 nozzles, (b) 19 nozzles and (c) 36 nozzles, were used.

Table 1
The physical properties of n-pentane at its saturation temperature at 1 bar.

Property	Values
Saturation temperature (°C)	36.0
Molar mass (kg/kmol)	72.15
Thermal diffusivity (m^2/s)	7.953×10^{-8}
Specific heat of liquid (kJ/kg K)	2.363
Specific heat of vapour (kJ/kg K)	1.66
Thermal conductivity of liquid (W/m K)	0.1136
Thermal conductivity of vapour (W/m K)	0.015
Kinematic viscosity (m^2/s)	2.87×10^{-7}
Viscosity (Pa s)	1.735×10^{-4}
Latent heat of vaporisation (kJ/kg)	359.1
Density of liquid (kg/m^3)	621
Density of vapour (kg/m^3)	2.89
Surface tension (N/m)	0.01432

The continuous phase system supply is made up of a 500 L constant temperature water bath with a temperature controller, water pump, pipes, fittings and valves. The water bath is heated by three electric heaters (3 kW each). The pressure in the water bath is controlled by a safety relief valve (1.5 bar operating pressure). Distilled water was used as the continuous phase. It was heated using a

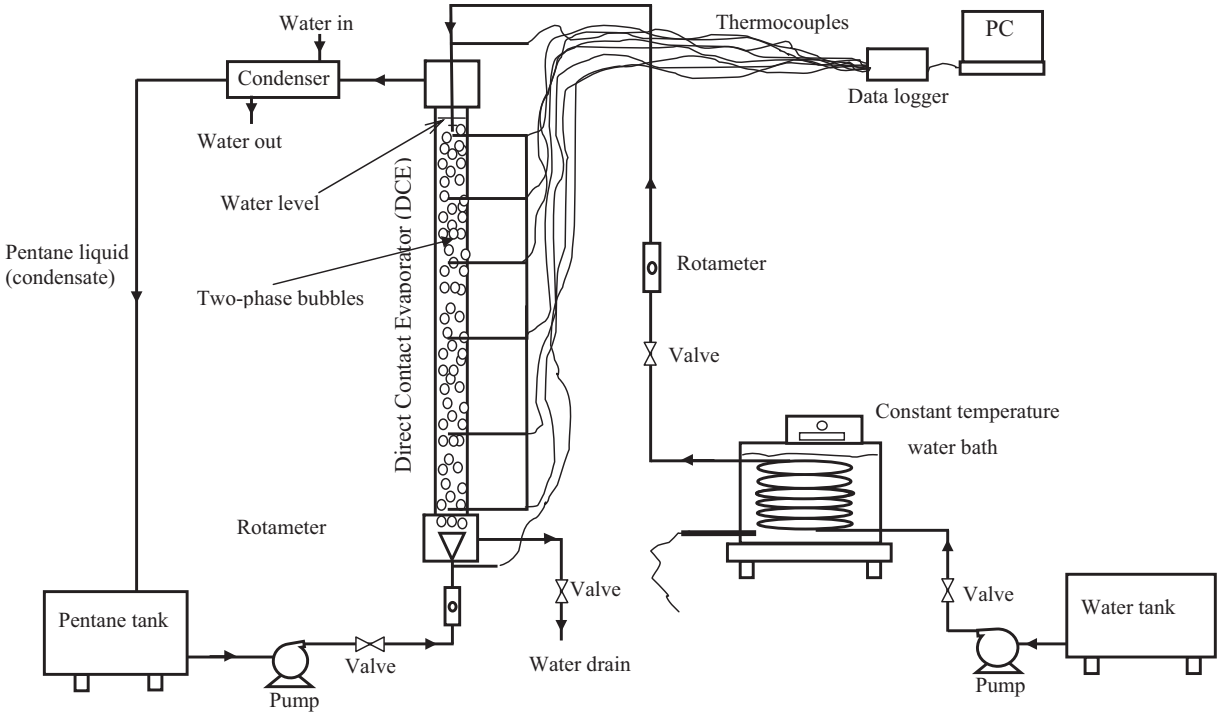

Fig. 1. Schematic diagram of the experimental rig.

10 mm outer diameter 2.5 m long copper coil which was completely immersed in the constant temperature water bath. The flow rate of both the dispersed phase and the continuous phase were measured before entering the test section using suitable rotameters with an error of ±1.25%.

Nine calibrated K-type thermocouples were used to measure the temperature distribution of the continuous phase along the test section and the inlet and outlet dispersed phase temperature. These thermocouples were connected to a 64 channel Data Logger (Delta-T Devices Ltd) and PC. A surface-type condenser was used to condense the dispersed phase vapour produced at the top of the test section during the experiments.

2.2. Experimental procedure

Once the continuous phase reached the temperature desired for the experimental run, it was circulated throughout the test section to maintain a constant temperature. The active height of the continuous phase was selected, and the temperature and the flow rate were measured. The dispersed phase (n-pentane liquid) at its saturation temperature was then injected into the test section via a sparger, at a specified flow rate. Pentane drops were formed at the sparger and then subsequently detached and rose up along the test section of the column. There was therefore counter-current contact between the dispersed phase moving up the column and the continuous phase moving down. Accordingly, the cold dispersed phase drops absorbed heat from the hot continuous phase and evaporated as they rose. Two-phase bubbles (liquid-vapour) formed (see Fig. 3) when the dispersed phase drops first come into direct contact with the continuous phase [31–35]. These bubbles consist of liquid n-pentane, which is immiscible with the aqueous continuous phase and the n-pentane vapour produced by evaporation. The two-phase bubbles existed along the majority of the column's height, and only become 100% vapour when they reached the end of the active height. The active height is the maximum section of the column over which the phase change of the dispersed phase drops occurred. After the pentane was evaporated, there remained a driving force for heat transfer to the bubbles, and so the vapour collected at the top of the column was in fact slightly superheated. As a consequence of the direct contact heat exchange, the continuous phase cools down while it moves down from the top of the column to the bottom. To perform the process as efficiently as possible the continuous phase should be drained out with minimum energy content. The continuous phase temperature profile was measured using the thermocouples and directly displayed on a PC via the data logger. The dispersed temperature was measured at only two points: the inlet and outlet. The vapour produced at the top of the column was condensed using a surface-type condenser and sent back to the dispersed phase storage tank to use again in another run. The conditions of the experiments are shown in Table 2.

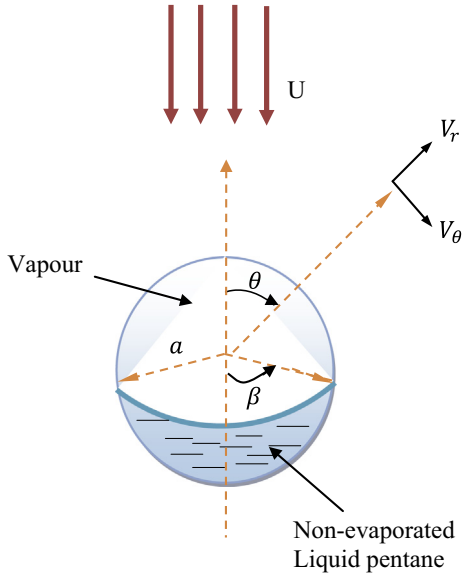

Fig. 3. Configuration of a two-phase bubble evaporating in an immiscible liquid (a represents the two-phase bubble radius, U denotes the continuous phase velocity, V_r and V_θ are the radial and tangential velocity components, θ is the angle in spherical coordinate).

3. Results and discussion

The local volumetric heat transfer coefficient along a three-phase spray column direct contact evaporator was studied experimentally. The calculation of the volumetric heat transfer coefficient was based on an energy balance, whilst assuming that latent heat dominated over sensible throughout the process. It was further assumed that there were no heat losses to the environment and that the flow rates of both the continuous and dispersed phases were constant. This is because of using a thick Perspex tube as a spray column, which is a poor conductor of heat, is likely to minimise the heat losses over the short duration of the experiments.

The local volumetric heat transfer coefficient can be found by:

$$U_{vi} = \frac{q_i}{A\Delta Z_i (\Delta T_{lm})_i} \tag{1}$$

where $(\Delta T_{lm})_i$, q_i, A and ΔZ_i denote the log-mean temperature difference for each sub-volume, the total heat transfer rate for each sub-volume, the direct contact condenser cross-sectional area and the height of a sub-volume, respectively.

The energy balance can be written as:

$$q_i = \dot{m}_c C_{pc} (T_{co} - T_{ci})_i = \dot{m}_{di} h_{fg} \tag{2}$$

where $\dot{m}_c$, is the mass flow rate of the continuous phase, C_{pc} is the specific heat capacity of the continuous phase, T_{co} and T_{ci} are the temperatures of the continuous phase as it leaves the and enters the sub-volume, $\dot{m}_{di}$ is the rate at which the dispersed phase evaporates in the sub-volume and hfg is the latent heat of vaporisation. The temperature difference between the contacting phases inevitably varies nonlinearly along the length of the column due to the effects of the nonlinear drop size distribution and back-mixing. This back-mixing is the main problem that hinders the direct contact heat exchanger. The use of the log-mean temperature difference accounts for these effects. For counter-current flow with latent heat dominating, the log-mean temperature difference is:

$$\Delta T_{lm} = \frac{(T_{ci} - T_{co})}{\ln\left(\frac{T_{ci} - T_d}{T_{co} - T_d}\right)} \tag{3}$$

Combining Eqs. (1)–(3) results in the local volumetric heat transfer coefficient:

Table 2
Conditions of experimental operations.

Temperature of the continuous phase (water) inlet	Temperature of the dispersed phase (n-pentane) inlet	Pressure at the top of test section	Volumetric flow rate of the continuous (water) phase	Volumetric flow rate of the dispersed (n-pentane) phase
45 °C ± 1%	36 ± 0.5%	1 atm	10–40 L/h ± 1.5%	10–20 L/h ± 1.5%

$$U_{vi} = \frac{\dot{m}_c C_{pc}}{A \cdot \Delta Z_i} \ln \left[\frac{(T_{co} - T_d)_i + \left(\frac{\dot{m}_{di}}{\dot{m}_c}\right) \frac{h_{fg}}{C_{pc}}}{(T_{co} - T_d)_i} \right] \quad (4)$$

where T_d denotes the temperature of the dispersed phase at each individual sub-volume (i.e. the saturation temperature).

It is well-known [6,7,10,12] that heat transfer in the direct contact device is dominated by transfer across the liquid-liquid interface. As the dispersed phase moves up the column, more vapour is produced within the two-phase bubble as a result of evaporation. Consequently, the liquid-liquid interface becomes smaller and the amount of energy that can be absorbed by the bubble as latent heat becomes lower. Therefore, the liquid fraction of the dispersed phase has to be specified along the column. By using the energy balance, the local non evaporated dispersed phase mass flow rate can be found using Eq. (2) above:

The evaporator height has been divided into six equally sized sub-volumes. From Eq. (4) above, only the outlet temperature of the continuous phase of each sub-volume and the mass flow rate of both phases are important to calculate the local volumetric heat transfer coefficient. Accordingly, the local temperature along the column height has been measured using thermocouples. The temperature of the dispersed phase was as assumed to be its saturation temperature.

3.1. Local volumetric heat transfer coefficient

The variation of the local volumetric heat transfer coefficient for three different sparger configurations and four different continuous phase flow rates is shown in Figs. 4 and 5. It is clear from the figures that the local volumetric heat transfer coefficient decreases monotonically upon moving up the exchanger. This is because of the decrease in the temperature driving force as the evaporating drops move upward, and the reduction of dispersed phase liquid to act as a heat sink. The decrease in the liquid content within the drops (i.e. the non-evaporated dispersed phase) as a result of evaporation also results in a reduction in the liquid-liquid interface. Thus, the internal heat transfer resistance in the drops increases because of the poor thermal conductivity of the vapour. Consequently, the local heat exchange and the local volumetric heat transfer coefficient are reduced.

The impact of the continuous phase flow rate on the local volumetric heat transfer coefficient is clearly demonstrated in Figs. 4 and 5. As expected, a higher continuous phase mass flow rate results in a higher volumetric heat transfer coefficient over the entire height of the exchanger. The continuous phase is the only the energy source that is responsible for the evaporation of the dispersed phase drops. A higher continuous phase flow rate means that there is sufficient energy which can be transferred to the dispersed phase drops and therefore the heat transfer coefficient of the process is increased, whilst the temperature difference between the contacting phases is maintained. It is also interesting to note that the effect of increasing the continuous phase flow rate on the volumetric heat transfer coefficient is lessened somewhat at higher flow rates. This effect is most evident at the lowest dispersed phase flow rate (10 L/h) in Figs. 4 and 5, but can be seen at the higher flow rates too. These observations would indicate that there are diminishing returns on increases in the continuous phase flow rate, with the optimum value depending on the dispersed phase flow rate. This is an important point to note when considering the most economic mode of operation for the exchanger.

The dispersed phase flow rate exhibits a similar effect on the volumetric heat transfer coefficient. This is more obvious at the bottom of the column as shown by Table 3 (Z = 5 cm at the bottom and Z = 65 cm at the top). This could be explained by the fact that at the bottom of the column, significant convective direct contact heat transfer between the two phases occurs. The heat exchange is slower higher up the exchanger due to the high internal heat transfer resistance that exists in the drop, which in turn reduces the impact of the dispersed phase flow rate. This is consistent with observations by Sideman and Taitel [36] for a single pentane drop evaporating in direct contact with hot water. They observed that a

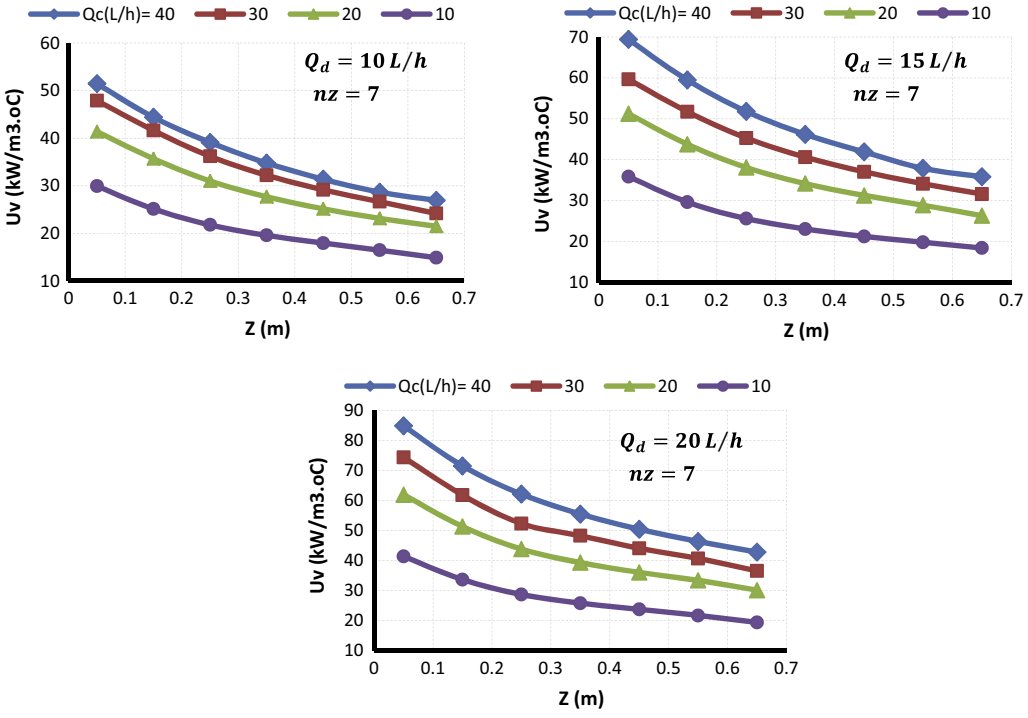

Fig. 4. Variation of the local volumetric heat transfer coefficient along the exchanger height for four different continuous phase mass flow rates and three dispersed phase flow rates for a sparger with 7 nozzles.

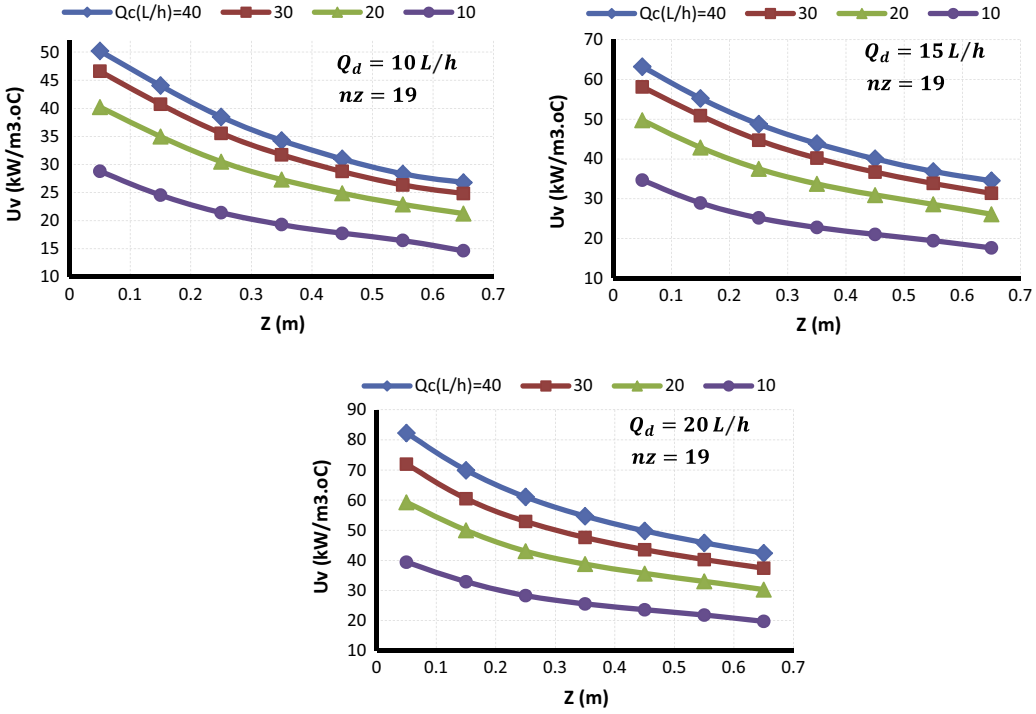

Fig. 5. Variation of the local volumetric heat transfer coefficient along the exchanger height for four different continuous phase flow rates and three dispersed phase flow rates for a sparger with 19 nozzles.

Table 3
The effect of the dispersed phase flow rate on the local volumetric heat coefficient at a point close to the injection point (Z = 5 cm) and near the top of the column (Z = 65 cm). Values for three different sparger configurations are shown.

Z (cm)	Q_c (L/h)	nz Q_d (L/h)	7 U_v	19 U_v	36 U_v
5	40	10	51.47	50.2	45.73
		15	69.42	63.22	60.69
		20	84.82	82.3	78.43
65	40	10	26.96	26.8	26.59
		15	35.83	34.52	34.27
		20	42.82	42.4	42.13

substantial proportion of a drop evaporated over only a short distance from the injection point.

The effect of the flow rates of the two phases on the average volumetric heat transfer coefficient can be clarified by considering the flow rate ratio as shown by Fig. 6 for two different sparger configurations. It is obvious from the figure that the volumetric heat transfer coefficient increases with increasing the flow rate ratio. This behaviour could be attributed to the fact that the increase in the mass flow rate ratio means an increase in the heating medium in the heat exchanger. Consequently, the heat transfer rate will rise due to the high energy content available.

It is also evident that the rate of increase of heat transfer coefficient with the flow rate ratio does decrease as the ratio increases. This is most likely because as the rate of the continuous phase is increased relative to the dispersed phase, the change in temperature of the continuous phase is smaller, hence there is less of a reduction in driving force for heat transfer. It is unclear whether an optimum value is approached asymptotically, or a true maximum is evident within the range of the flow rate ratios used.

The uncertainty in estimates of the volumetric heat transfer coefficient was calculated using the method suggested by Coleman and Steele [37]. The results indicate that the uncertainty strongly depends on the error in the continuous mass flow rate rather than

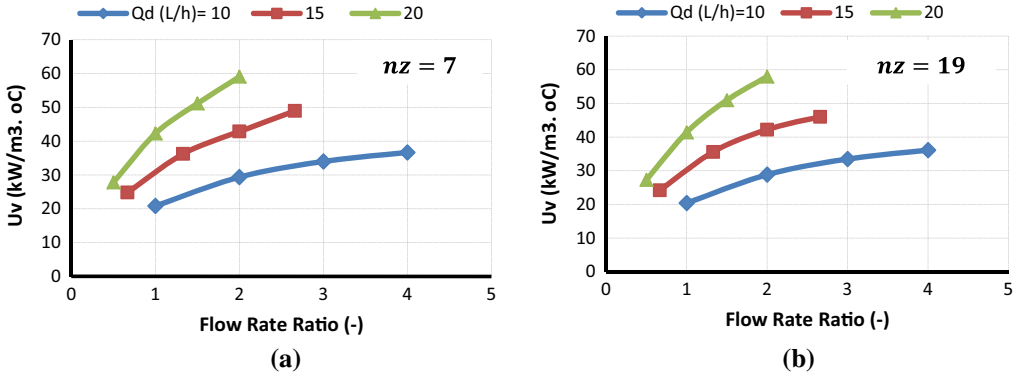

Fig. 6. Variation of the average volumetric heat transfer coefficient with flow ratio of the continuous phase and dispersed phase for two different sparger configurations (a) 7 nozzles and (b) 19 nozzles.

the other parameters, such as dispersed phase mass flow rate and log-mean temperature difference. However, the maximum uncertainty was found about ±3%.

The effect of the sparger configuration on the local volumetric transfer coefficient of the exchanger for three different dispersed phase flow rates was studied and the pertinent results are presented in Fig. 7. The local volumetric heat transfer coefficient does show a slight decrease when the number of nozzles in the sparger is increased. This is especially apparent near the bottom of the column. Towards the top of the column the differences between the heat transfer coefficient for different nozzle numbers effectively vanishes. This can be explained by the fact that at the same dispersed phase flow rate and nozzle diameter, the dispersed phase injection velocity is increased when there are fewer nozzles in the sparger. Consequently, a smaller two-phase bubble is formed at the sparger because the drop/bubble formation time is shortened, and the velocity relative to the continuous phase is increased. Therefore, the convective heat exchange between the two phases is increased. Towards the top of the column the motion of the bubbles is dominated by buoyancy forces and so the effect of the injection velocity on the heat transfer is substantially lessened. What these results clearly show is that the injection velocity and hence bubble formation significantly affects the heat transfer in the three-phase direct contact heat exchanger. This is in accord with that has been found by Mahood [38]. He recommended that the two-phase bubble velocity is the most important factor that must be incorporated directly or indirectly in any quantitative description of heat transfer in a three-phase direct contact exchanger.

Fig. 7 also clearly shows a significant increase in the local volumetric heat transfer coefficient when the dispersed phase flow rate is increased. As mentioned above, the higher dispersed phase flow rate can enhance the heat transfer process due to the increased interfacial area and the higher relative velocities of the phases.

In addition to the number of nozzles in the sparger affecting the performance, it is likely that the diameter of the nozzles will also have an effect. In Fig. 8 is presented a comparison of the local volumetric heat transfer coefficient along the direct contact exchanger for two different nozzle diameters and so two different nozzle Reynolds numbers. It is once again evident that regardless of the dispersed and continuous phase flow rates, the local volumetric heat transfer coefficient decreases slightly when the nozzle Re_o (nozzle diameter) is decreased from 1760 to 1410), which corresponding to the change in the nozzle diameter from 1 mm to 1.25 mm. In fact, the increase in the nozzle Re_o results in an increase in the dispersed phase drops injection velocity, which

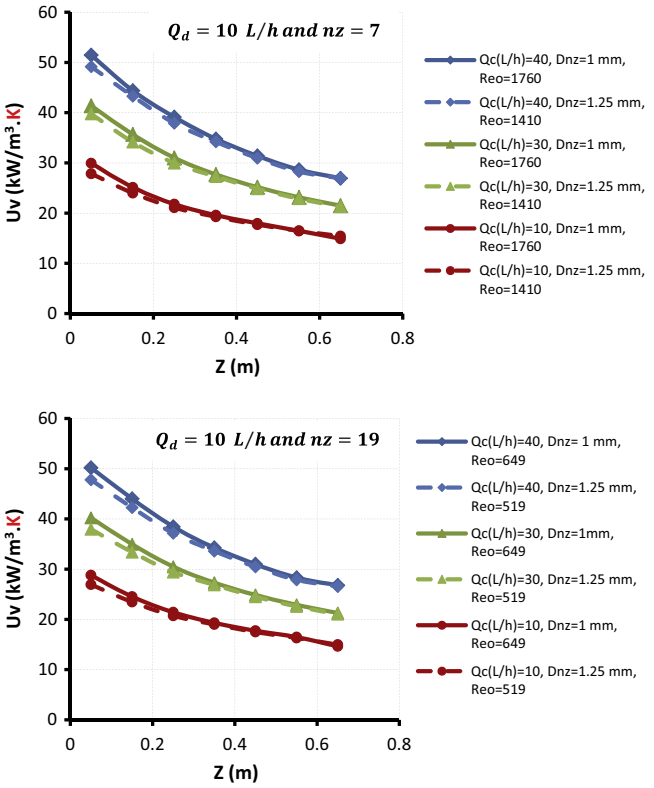

Fig. 8. The effect of the diameter of the nozzles in the sparger on the local volumetric heat transfer coefficient along the exchanger height for three different continuous phase flow rates.

enhances the volumetric heat transfer coefficient [17]. This could be due to the improved mixing caused by the faster moving drops as well as the reduction in thickness of the boundary layer surrounding the drops. At the same time, the increase in the diameter of the nozzles significantly influenced the drop size, which affected the interfacial heat transfer area. The larger nozzle diameter, the larger the drop size, and hence the lower the heat transfer area [30]. This results in a low heat transfer rate.

Fig. 9 shows the effect of the continuous phase temperature in terms of Jacob number (*Ja*) on the average volumetric heat transfer coefficient of the heat exchanger, for three different sparger configurations and dispersed phase flow rates. The continuous phase *Ja* was calculated as:

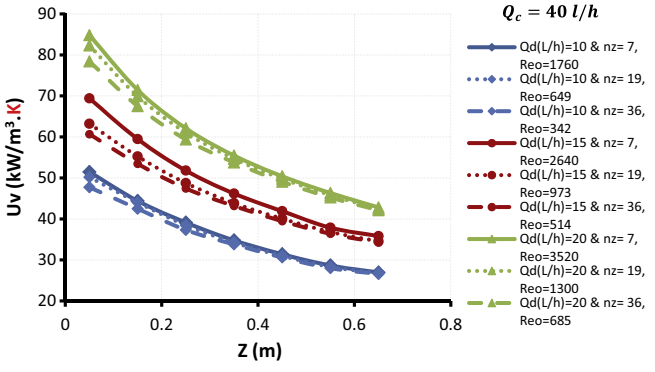

Fig. 7. The effect of sparger configuration on the local volumetric heat transfer coefficient. The variation of the heat transfer coefficient with height in the column is shown for three different dispersed phase flow rates and for spargers with 7, 19 or 36 nozzles.

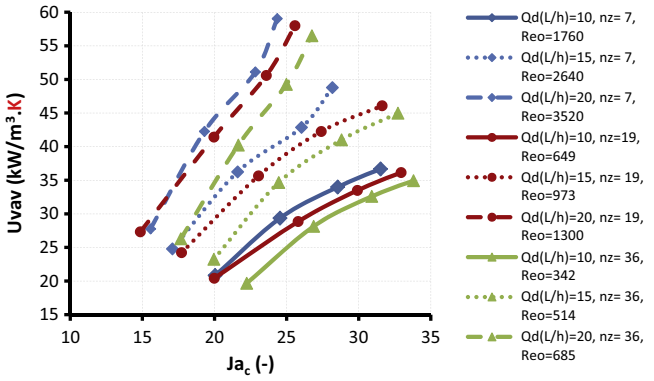

Fig. 9. Effect of the continuous phase Jacobs number on the average heat transfer coefficient for three different dispersed phase flow rate and three different nozzle configurations.

$$Ja = \frac{\rho_c C_{pc}(T_c - T_d)}{\rho_v h_{fg}} \quad (5)$$

In general, the average volumetric heat transfer coefficient was found to increase with *Ja*. The temperature difference, in fact, represents the main driving force that drives the direct contact heat transfer process. Accordingly, increasing the driving force (ΔT) increases the heat exchange between the two phases and of course increases the volumetric heat transfer coefficient, which enhances the performance of the heat exchanger. Similar to above findings, the increase in the dispersed phase flow rate results in an increase in the average volumetric heat transfer coefficient. Again, the increase of number of nozzles in the sparger results in a reduction in the average volumetric heat transfer coefficient.

3.2. Heat exchanger active height

The active height can be simply defined as the minimum height of the continuous phase in the column that can lead to a complete evaporation of the dispersed phase drops. Therefore, it directly affects the cost of the heat exchanger by influencing its volume. Also, the hydrostatic pressure variation would be increased with an increase of the active height, which would result in a reduction in the mixing rate [39]. Fig. 10 shows the variation of the heat exchanger active height with the continuous flow rate at three different dispersed phase flow rates. For a constant dispersed phase flow rate and sparger configuration, the active height was found to decrease with the continuous flow rate. This could be explained by the fact that at the higher continuous phase flow rate, the amount of energy available in the heat exchanger is adequate to completely evaporate the dispersed drops over a very short distance from the injection point. On the other hand, at a constant continuous phase flow rate the active height was significantly affected by an increase in the dispersed phase flow. The higher the dispersed phase flow rate, the higher the heat exchanger active height. This is because the increase flow of the dispersed phase requires a larger volume of the continuous phase for complete evaporation of the drops.

The sparger configuration was found to have a significant effect on the active height of the heat exchanger. As shown by Fig. 11 the active height was significantly increased by increasing the number of nozzles in the sparger. As mentioned above, this could be as a result of the slower heat transfer between the drops and the hot water.

Finally, the effect of the temperature driving force, as characterised by the Jacob number (*Ja*), on the active height was studied and is shown in Fig. 12, for three different dispersed phase flow rates. The dependency of the active height on *Ja* was similar to that already found for the case of the effect of the continuous phase flow rate on the active height, (Fig. 10). It is obvious that the energy content of the continuous phase increases with its flow rate. Therefore, the temperature driving force is increased accordingly. The amount of energy available in the continuous phase still high whatever how much the dispersed phase absorbed. Also, it is clear from the figure, that the active height is significantly affected by the dispersed phase flow rate. The higher the dispersed phase flow rate, the higher the active height. This is as expected, where the higher dispersed phase flow rate needs more energy for complete evaporation.

4. Conclusions

In the present study, the local volumetric heat transfer coefficient and the active height of a spray column direct contact heat exchanger were measured. The experimental study was performed under various operating conditions; specifically, the continuous phase flow rate, dispersed phase flow rate, sparger configuration and temperature difference between the contacting fluids were all varied. With these data, the performance of the spray column direct contact heat exchanger under the influence of various operational conditions was obtained. The results show that the flow rate of the dispersed phase has more pronounced effect on U_v than that of the continuous phase and both phases flow rates have positively influenced U_v. The influence of both phases, however, becomes more obvious at high flow rates of the two phases. The

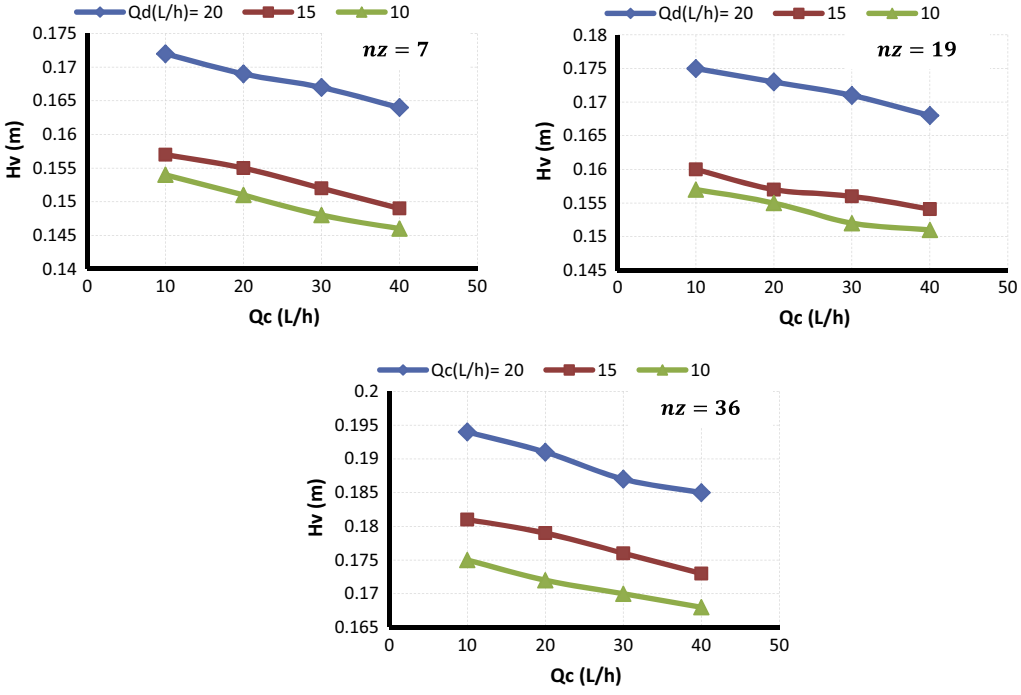

Fig. 10. The variation of active height with the continuous flow rate for different dispersed flow rates and sparger configurations.

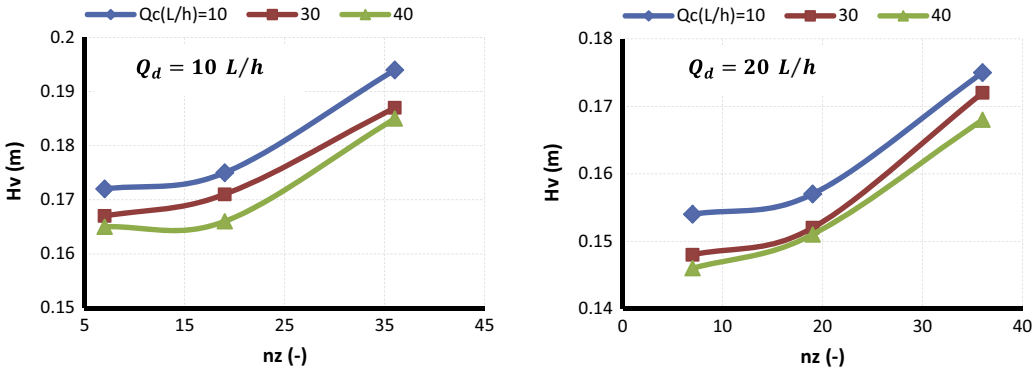

Fig. 11. The variation of the active height with the continuous flow rate for different dispersed flow rates and sparger configurations.

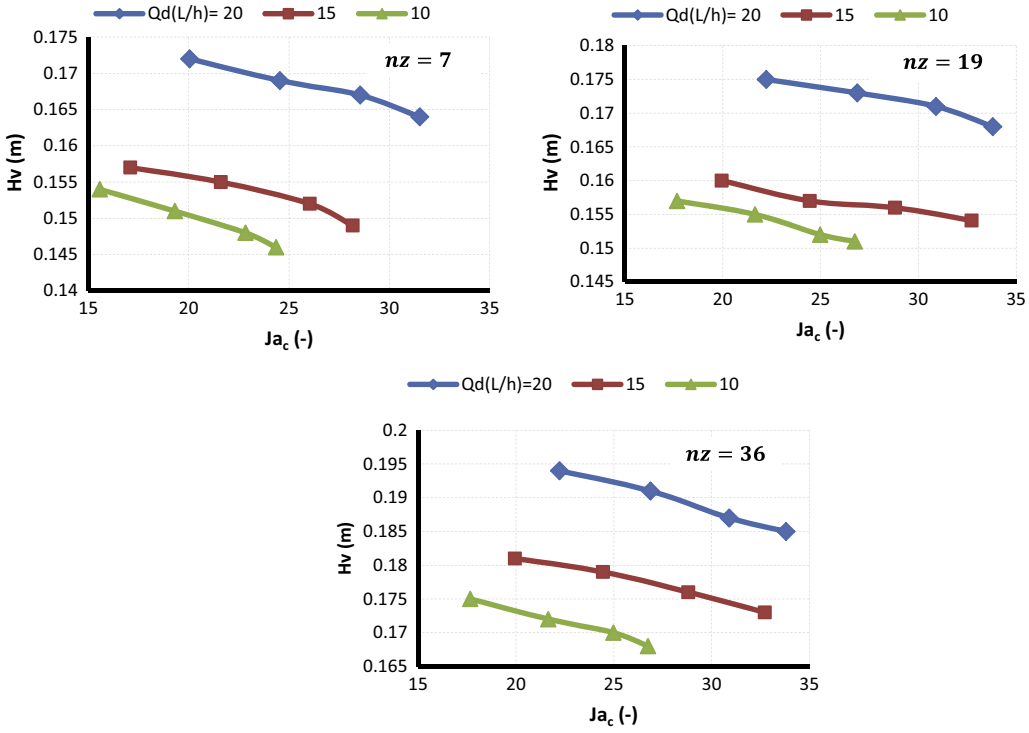

Fig. 12. Variation of active height with the continuous phase Jacob number for different dispersed and three different sparger configurations.

maximum average U_v was 59.05 kW/m^3 K at continuous and dispersed phase flow rates of 40 L/h and 20 L/h, respectively. The number of nozzles in the sparger has no significant impact on the average U_v. The U_v was 59.05, 58.0 & 56.5 kW/m^3 K for nz = 7, 19 & 36 respectively, with the same above flow rates of the continuous and dispersed phases. The local volumetric heat transfer coefficient was inversely affected by increasing the diameter of the injecting nozzle and number of nozzles in the sparger. In both cases this resulted in a reduction in Re for the injection of the dispersed phase. The lower relative velocity of the injection leads to a lower rate of convective heat transfer, as one would expect intuitively. The temperature driving force in term of *Ja* had a significant positive impact on the volumetric heat transfer coefficient. This impact was significant at a high dispersed phase flow rate, where U_v varied almost linearly with *Ja* and the maximum average U_v nearly doubled It was changed from 27.78 to 59.06 kW/m^3 K, 27.337–58.0 kW/m^3 K and 26.3–56.6 kW/m^3 K, when Q_d = 20 L/h and for nz = 7, 19 & 36, respectively.

Furthermore, the results indicated that the active height of heat exchanger was significantly affected by the flow rate of both phases. The higher the continuous or dispersed phase, the lower the active height of the exchanger for a similar effect was observed for the temperature driving force, while the number of injecting nozzle had the opposite effect.

In summary, with the absence of adequate data or theoretical results, the present experimental results could be helpful in the design of spray column direct contact heat exchangers. These data could help to improve the operational method in order to produce an efficient and low cost spray column direct contact heat exchanger for utilising in energy recovery from low-grade resources.

References

[1] Mahood HB, Campbell AN, Thorpe RB, Sharif AO. Heat transfer efficiency and capital cost evaluation of a three-phase direct contact heat exchanger for the utilisation of low-grade energy sources. Energy Convers Manage 2015;106:101–9.

[2] Baqir ASh. Theoretical and experimental study of direct-contact evaporation of a volatile drops(n-pentane) in an immiscible liquid (distilled water) PhD Thesis. Iraq: Dep. Mechanical Engineering, University of Basrah; 2010.
[3] Wright JD. Selection of a working fluid for an organic Rankine cycle coupled to a salt-gradient solar pond by direct-contact heat exchange. J Sol Energy Eng 1982;104(4):286–92.
[4] Mahood HB, Thorpe RB, Campbell AN, Sharif AO. Experimental measurements and theoretical prediction for the transient characteristic of a three-phase direct contact condenser. Appl Therm Eng 2015;87:161–74.
[5] Hewitt GF, Shires GL, Bott RT. Process heat transfer. CRC Press Inc.; 1993.
[6] Sideman S, Gat Y. Direct contact heat transfer with change of phase: spray column studies of a three-phase heat exchanger. AIChE J 1966;12(2):296–303.
[7] Mori YH. An analytic model of direct-contact heat transfer in spray-column evaporators. AIChE J 1991;37(4):539–46.
[8] Bauerle GL, Ahlert RC. Heat transfer and holdup phenomena in spray column. Indus Eng Chem Pro Desg Devl 1965;4(2):225–30.
[9] Plass SB, Jacobs HR, Boehm RF. Operational characteristics of a spray column type direct contact contactor preheater. In: AIChE symposium series-heat transfer, vol. 75, no. 89, 1979. p. 227–34.
[10] Sideman S, Hirsch G, Gat Y. Direct contact heat transfer with change phase: effect of the initial drop size in three-phase heat exchanger. AIChE J 1965;11(6):1081–7.
[11] Coban T, Boehm R. Performance of a three-phase, spray -column, direct-contact heat exchanger. J Heat Trans 1989;111(1):166–72.
[12] Jacobs HR, Golafshani M. Heuristic evaluation of the governing mode of heat transfer in a liquid-liquid spray column. J Heat Trans 1989;111(3):773–9.
[13] Shimizu Y, Mori YH. Evaporation of single liquid drops in an immiscible liquid at elevated pressure: experimental study with n-pentane and R113 drops in water. Int J Heat Mass Trans 1988;31(9):1843–51.
[14] Battya P, Raghavan VR, Seetharamu KN. Parametric analysis of direct contact sensible heat transfer in spray column. Lett Heat Mass Trans 1982;9(4):265–76.
[15] Core KL, Mulligan JC. Heat transfer and population characteristics of dispersed evaporating droplets. AIChE J 1990;36(8):1137–44.
[16] Summers SM, Crowe CT. One-dimensional numerical model for a spray column heat exchanger. AIChE J 1991;37(11):1673–9.
[17] Brickman RA, Boehm RF. Maximizing three-phase direct contact heat exchanger output. Num Heat Trans, Part A Appl 1994;26(3):287–99.
[18] Tadrist L, Sun J, Santini R, Pantaloni J. Heat transfer with vaporization of a liquid by direct contact in another immiscible liquid: experimental and numerical study. J Heat Trans 1991;113(3):705–13.
[19] Siqueiros J, Bonilla O. An experimental study of a three-phase, direct-contact heat exchanger. Appl Therm Eng 1999;19(5):477–93.
[20] Mahood HB, Sharif AO, Hossini SA, Thorpe RB. Analytical modelling of a spray column three-phase direct contact heat exchanger. ISRN Chem Eng 2013. http://dx.doi.org/10.1155/2013/457805 457805.
[21] Wang Y, Fu H, Huang Q, Cui Y, Sun Y, Jiang L. Experimental study of direct contact vaporization heat transfer on n-pentane-water flowing interface. Energy 2015;93:854–63.
[22] Jian Y, Huang Q, Wang Y, Cui Y, Fu H. The effect of Dixon rings on direct contact evaporative heat transfer performance. Appl Therm Eng 2015;87:336–43.
[23] Mahood HB, Sharif AO, Al-aibi S, Hwakis D, Thorpe RB. Analytical solution and experimental measurements for temperatures distribution prediction of three-phase direct contact condenser. J Energy 2014;67:538–47.
[24] Mahood HB, Sharif AO, Thorpe RB. Transient volumetric heat transfer coefficient prediction of a three-phase direct contact condenser. J Heat Mass Transf 2015;51(2):165–70.
[25] Mahood HB, Campbell AN, Thorpe RB, Sharif AO. Experimental measurements and theoretical prediction for the volumetric heat transfer coefficient of a three-phase direct contact condenser. Int Comm Heat Mass Trans 2015;66:180–8.
[26] Mahood HB, Campell AN, Sharif AO, Thorpe RB. Heat transfer measurement in a three-phase direct contact condenser under flooding conditions. Appl Therm Eng 2016;95:106–14.
[27] Mahood HB, Thorpe RB, Campbell AN, Sharif A. Effect of various parameters on the temperature measurements in a three-phase direct contact condenser. Int J Therm Tech 2015;5(1):23–7.
[28] Mahood HB, Sharif A, Thorpe BR, Campbell AN. Heat transfer measurements of a three-phase direct contact condenser for application in energy production and water desalination. In: The 3rd int conf on water, energy and env, Sharjah, AUS, 24–27 March 2015.
[29] Mahood HB, Campbell AN, Thorpe RB, Sharif A. A new model for the drag coefficient of a swarm of condensing vapour–liquid bubbles in a third immiscible liquid phase. Chem Eng Sci 2015;131:76–83.
[30] Baqir ASh, Mahood HB, Campbell AN, Griffiths AJ. Measuring the average volumetric heat transfer coefficient of a liquid-liquid-vapour direct contact heat exchanger. Appl Therm Eng 2016;103:47–55.
[31] Sideman S, Taitel Y. Direct-contact heat transfer with change of phase: evaporation of drops in an immiscible liquid medium. Int J Heat Mass Transf 1964;7:1273–89.
[32] Sideman S. Direct contact heat transfer between immiscible liquids. Adv Chem Eng 1966;6:207–86.
[33] Shimizu Y, Mori YH. Evaporation of single liquid drops in an immiscible liquid at elevated pressures: experimental study with n-pentane and R 113 drops in water. Int J Heat Mass Transf 1988;31(9):1843–51.
[34] Simpson HC, Beggs GC, Nazir M. Evaporation of a droplet of one liquid rising through a second immiscible liquid. A new theory of the heat transfer process. Heat Transf 1974(5):59–68.
[35] Simpson H, Beggs G, Nazir M. Evaporation of butane drops in brine. Desalination 1974;15(1):11–23.
[36] Sideman S, Taitel Y. Direct-contact heat transfer with change of phase: evaporation of drops in an immiscible liquid medium. Int J Heat Mass Transf 1964;7(11):1273–89.
[37] Coleman HW, Steele WG. Experimentation and uncertainty analysis for engineers. New York: John Wiley & Sons; 1999.
[38] Mahood HB. Experimental and theoretical investigation of a three-phase direct contact condenser PhD Thesis. UK: Dept. of Chemical and Process Engineering, University of Surrey; 2015.
[39] Abdulrahman MW. Experimental studies of direct contact heat transfer in a slurry bubble column at high gas temperature of a helium-water-alumina system. Appl Therm Eng 2015;91:515–24.